HUMAN-ROBOT INTERACTION

Neglected physical human-robot interaction may explain variable outcomes in gait neurorehabilitation research

M. Plooij[1,2,3†], S. Apte[1,4†], U. Keller[5,6,7], P. Baines[1], B. Sterke[3,8], L. Asboth[9,10,11], G. Courtine[5,9,10,11], J. von Zitzewitz[5,6‡], H. Vallery[1,8,*‡]

During gait neurorehabilitation, many factors influence the quality of gait patterns, particularly the chosen body-weight support (BWS) device. Consequently, robotic BWS devices play a key role in gait rehabilitation of people with neurological disorders. The device transparency, support force vector direction, and attachment to the harness vary widely across existing robotic BWS devices, but the influence of these factors on the production of gait remains unknown. Because this information is key to designing an optimal BWS, we systematically studied these determinants in this work. We report that with a highly transparent device and a conventional harness, healthy participants select a small backward force when asked for optimal BWS conditions. This unexpected finding challenges the view that during human-robot interactions, humans predominantly optimize energy efficiency. Instead, they might seek to increase their feeling of stability and safety. We also demonstrate that the location of the attachment points on the harness strongly affects gait patterns, yet harness attachment is hardly reported in literature. Our results establish principles for the design of BWS devices and personalization of BWS settings for gait neurorehabilitation.

INTRODUCTION

Stroke, spinal cord injury (SCI), or other neurological disorders lead to locomotor impairments affecting quality of life. Intensive gait neurorehabilitation can improve the recovery of locomotor function, especially when the affected individuals engage in intense training programs that challenge their movement repertoire in conditions that closely resemble their natural environment (*1*). The first priority of gait neurorehabilitation therapies is safety. Safe conditions not only prevent injuries but also enable users to constantly push their own limits (*2*). The second priority is to establish optimal conditions that produce gait patterns as physiologically normal as possible (*3*). Because of weakness and neuromuscular impairment, most patients with neurological disorders produce improved gait patterns (*4*, *5*) when their body weight (BW) is partially supported. The third priority is to establish ecological conditions (*6*, *7*) to train the entire repertoire of natural locomotor activities underlying daily living.

Requirements for safety, optimal body-weight support (BWS), and natural walking conditions can be addressed with active multidirectional overground BWS devices. This understanding triggered the development of various robotic BWS systems with very different properties.

The first active support system for overground walking was Zero-G (*8*), which runs on rails attached to the ceiling and controls the force vector in both vertical and walking directions. However, horizontal force components orthogonal to the walking direction [mediolateral (ML) forces] are important for dynamic balance during neurorehabilitation (*9*). Support systems relying on single rails impose horizontal forces that resemble a pendulum, which drastically reduces the challenge for balance maintenance (*10*). Instead, free balance training during gait neurorehabilitation relies on low impedance, which requires high device transparency in the lateral direction. Haptic transparency, originally coined in the domain of teleoperation, describes the ability of an interface to render a desired physical impedance, i.e., a force response to an input velocity, with high fidelity (*11*). For a reference impedance of zero, transparency is therefore equivalent to rendering only negligible forces in response to user movement. For this reason, an emerging generation of robotic BWS devices, such as FLOAT (*12*) and RYSEN (*13*), incorporates adjustable support force in the ML direction. Because the investigations here are based on these two systems, we introduce and compare them in more detail in Fig. 1. Using FLOAT, we previously showed that patients with SCI or stroke produce optimal gait patterns when the BWS is precisely personalized to each patient's needs. We also reported that finely calibrated anteroposterior (AP) forces are required to compensate for the influence of vertical BWS on body posture (*9*). These results stress the importance of understanding the precise determinants for optimal BWS conditions during gait neurorehabilitation.

Numerous studies have investigated the influence of BWS on gait patterns, and the results are less consistent than one would expect (*14*). This variability reflects the numerous determinants affecting gait (Fig. 1), including the specific features of BWS (D1 to D3), user (D4 and D5), and environment (D6 to D9). See table S3 for definitions of the determinants.

[1]Department of Biomechanical Engineering, Delft University of Technology, Mekelweg 2, 2628 CD Delft, Netherlands. [2]Demcon Advanced Mechatronics, Delfttechpark 23, Delft, Netherlands. [3]Motek, a DIH brand, Hogehilweg 18-C, 1101 CD Amsterdam, Netherlands. [4]Laboratory of Movement Analysis and Measurement, École Polytechnique Fédérale de Lausanne (EPFL), Lausanne, Switzerland. [5]ONWARD, EPFL Innovation Park, Lausanne, Switzerland. [6]Center for Neuroprosthetics (CNP) Valais, École Polytechnique Fédérale de Lausanne (EPFL), Lausanne, Switzerland. [7]Swiss Children's Rehab, University Children's Hospital Zurich, Affoltern am Albis, Switzerland. [8]Department of Rehabilitation Medicine, Erasmus MC, Postbus 2040, 3000 CA Rotterdam, Netherlands. [9]Center for Neuroprosthetics and Brain Mind Institute, School of Life Sciences, École Polytechnique Fédérale de Lausanne (EPFL), Lausanne, Switzerland. [10]Department of Clinical Neuroscience, Lausanne University Hospital (CHUV) and University of Lausanne (UNIL), Lausanne, Switzerland. [11]Defitech Center for Interventional Neurotherapies (NeuroRestore), EPFL/CHUV/UNIL, Lausanne, Switzerland.
*Corresponding author. Email: h.vallery@tudelft.nl
†These authors contributed equally to this work as co–first authors.
‡These authors contributed equally to this work as co–last authors.

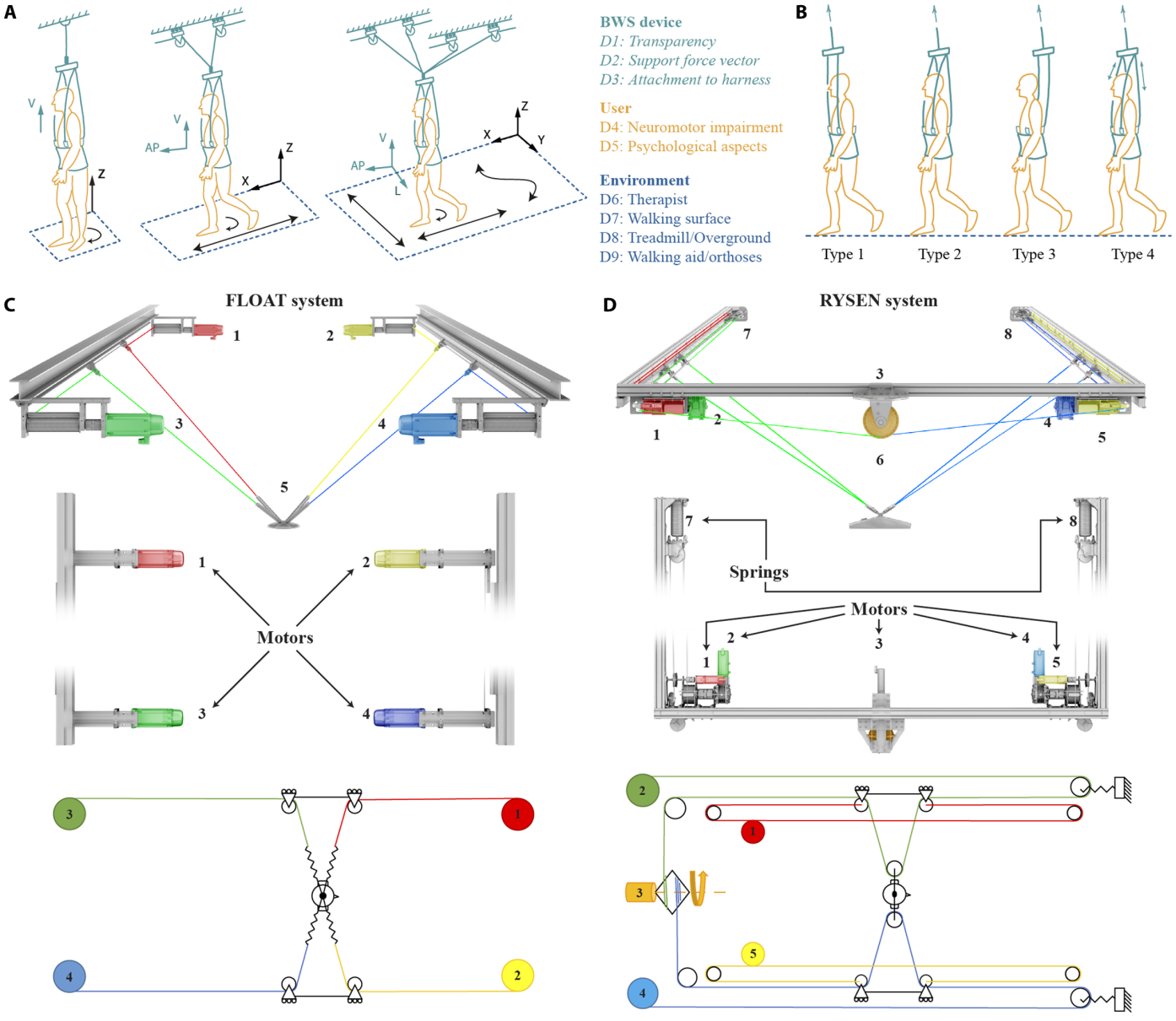

Fig. 1. Characterization of BWS systems and their influence on gait. (**A**) Illustration of the DOFs of BWS systems and a nonexhaustive overview of determinants influencing gait parameters (emphasized in italic are the ones investigated in this paper). (**B**) Attachment types that are tested: only front attached (type 1), front and back attached (type 2), back attached (type 3), and looped (type 4). (**C** and **D**) Renderings of the two 3D BWS systems FLOAT (C) and RYSEN (D). FLOAT relies on four identical direct-drive high-power motors that each connect to the sling bar via a dedicated cable. In contrast, RYSEN uses five different-sized geared motors and a sling bar that travels along two shared cables, which allows almost completely decoupled DOFs and a reduction in power consumption.

Here, we study the determinants linked to the properties of robotic BWS devices: device transparency (D1), support force vector (D2), and attachment to the harness (D3). Principles from the domains of humanoid robotics and physical human-robot interaction lend themselves to shed a clearer light on the influence of these factors.

Transparency of a robotic device (D1) relates to its capability to render a reference physical impedance in haptic interaction with a human, without exhibiting any further undesired interaction forces. Such parasitic forces are generally unavoidable due to any robot's bandwidth limitations and stability constraints prohibiting high feedback gains (*15*). They can be mitigated up to a certain point by appropriate hardware and control design (*16*). Still, their presence may cause artifacts that sometimes even occlude the main effects to be studied, so their quantification is important for data interpretation. Transparency has been thoroughly investigated for upper-limb rehabilitation robots, as evinced by several reviews (*17*–*19*). However, few papers address transparency of robotic BWS (*20*), complicating comparisons between devices. Here, we compare the transparency of the two commercial state-of-the-art three-dimensional (3D) BWS systems, FLOAT and RYSEN.

The direction of the support force vector (D2), i.e., the relationship between upward and forward forces, influences a person's ability

to walk. We recently showed that even small changes in forward forces can drastically change walking velocity (*9*). However, we had not yet separated the influence of intentional, therapist-determined reference forces from artifacts related to low device transparency (D1).

Whole-body centroidal angular momentum (*21*), a proxy for bipedal stability, depends on the sum of external moments about the body's center of mass. The harness attachment (D3) determines the point of application of the resultant force, and thereby also angular momentum. However, attachment not only influences the moment arm about the center of mass but also individual joint moments. Because the force applies only at the upper body and not in a distributed fashion, it alters biomechanics drastically—as we will show, up to the point where signs of required joint moments for a given posture may flip.

These three determinants have not yet been conclusively studied for robotic BWS. From the 55 studies we covered in a recent review (*14*), only one study systematically investigated the influence of harness attachment (D3), and only three publications studied transparency (D1) of BWS systems in a systematic way and in dynamic walking conditions. Although 14 papers studied the fluctuations (peak and mean) in the vertical unloading force, they did not investigate backward/forward forces (D2) on the user that can be generated due to the attaching cable not being vertical. Clinical studies (*22*–*28*) on the effectiveness of BWS treadmill training (BWSTT) typically have not reported D1 and D3, which hindered systematic reviews (*29*–*32*) in controlling for the determinants in their inclusion/exclusion criteria or risk-of-bias assessments. This phenomenon may explain the mixed results of these studies, where four of seven original articles showed BWSTT to be more effective, but only one of four review papers confirmed it.

Using both FLOAT (Lutz Medical Engineering, Switzerland) and RYSEN (Motek Medical, The Netherlands) devices in healthy participants and patients with SCI, we show that these three determinants (D1 to D3) change the way data from previous studies should be interpreted. Our results will affect the design of optimal BWS devices and personalization of BWS therapy for gait neurorehabilitation.

RESULTS

D1: Device transparency

It seems obvious that the physical impedance a device displays influences the way users physically interact with it. Mechanical impedance can be characterized in the frequency domain by a frequency-dependent gain and phase shift between the input velocity and the force response. Mechanical impedance can be further approximated by apparent mass, damping, and stiffness. It is not possible to render precisely zero impedance in any physically realizable device (*15*), although inserting physical compliance, which is done in both FLOAT and RYSEN, can be particularly effective (*33*). This limits achievable transparency, i.e., the ability of rendering a desired impedance with high fidelity. Inherent system properties such as inertia and friction, in combination with the implemented controller, determine the apparent impedance of a robotic device. In some training regimes, a nonzero impedance might even be desirable, for example, adding resistance in the form of a damping or stiffness to improve the feeling of safety. However, to accurately and precisely track a desired constant force vector, which is a frequent use case, minimal impedance needs to be rendered, requiring high device transparency.

The transparency of FLOAT was assessed in (*20*). Here, we revisit FLOAT transparency on another specimen, and juxtapose data collected with RYSEN using a dedicated test setup and with participants walking in it. This addresses our first research question:

1) What is the transparency of state-of-the-art 3D BWS systems?

We evaluated force tracking performance with participants walking in the system, as well as the frequency response and remaining impedance with a dedicated setup. Furthermore, we investigate transparency of RYSEN in more detail. These results are crucial when assessing and attempting to generalize the results of the other two determinants discussed later.

1. What is the transparency of state-of-the-art 3D BWS systems?

The transparency of RYSEN was assessed with two experiments, and we extracted part of analogous transparency data for FLOAT from previous experiments (*9*). All transparency results are shown in device coordinates. The *x* direction (see Fig. 1) aligns with the direction of walking (AP direction) for most use cases. We let 16 healthy participants walk at self-selected velocity with a BWS between 10 and 60%, in combination with AP forces between −3 and +6% of their BW (% BW). Figure 2 (A to C) shows the force tracking performance of RYSEN during these experiments, in terms of variability and bias. We also measured the force tracking errors in the *x* direction during walking, in both RYSEN and FLOAT. Figure 2D shows these errors as functions of walking velocity. This shows that the controller errors in FLOAT are at least an order of magnitude larger than those in RYSEN. For instance, walking at 1 m/s in the *x* direction in RYSEN with 200-N unloading leads to about −1-N bias of the force in the *x* direction, whereas the same condition in FLOAT leads to a bias of about −83 N. In both cases, the internal sensors of the devices were used, so these values include measurement biases. In the case of RYSEN, we further quantified the absolute measurement biases for the *y* and *z* directions to range from 12 to 15 N (see Table 2).

In the second experiment, we assessed the transparency in all directions by letting one participant walk figures of 8 with 10% (70 N), 30% (210 N), and 60% (420 N) unloading and no horizontal force. Because the force seemed to depend mainly on the velocity, we fitted a damper model on the velocity-force data of those experiments. In the *x* direction, the fitted damping parameters ranged between 2 and 3 Ns/m. In the *y* direction, the fitted damping parameters were 24, 28, and 45 Ns/m for the three levels of BWS. In the *z* direction, fitted damping parameters ranged from 288 to 297 Ns/m. See Table 1 for an overview of the results and a comparison between RYSEN and FLOAT.

For a technical verification of the transparency of RYSEN, we analyzed the frequency response and the linearized remaining impedance. Figure S3 shows the frequency response of RYSEN to reference forces. The force control bandwidth, measurement errors, and tracking errors are listed in Table 2. We also fitted a linear mass-spring-damper-bias model to disturbance experiments data, with model parameters listed in Table 2.

D2: Support force vector

Previously, we showed that the magnitude of the rendered AP force needs to be finely tuned to the vertical force and the walking velocity (*9*). However, we had not yet separated device- and attachment-dependent effects from participant-dependent effects. Therefore, we replicate our FLOAT-based experiments with a different robotic system, RYSEN, which (as the results on D1 showed) is more transparent

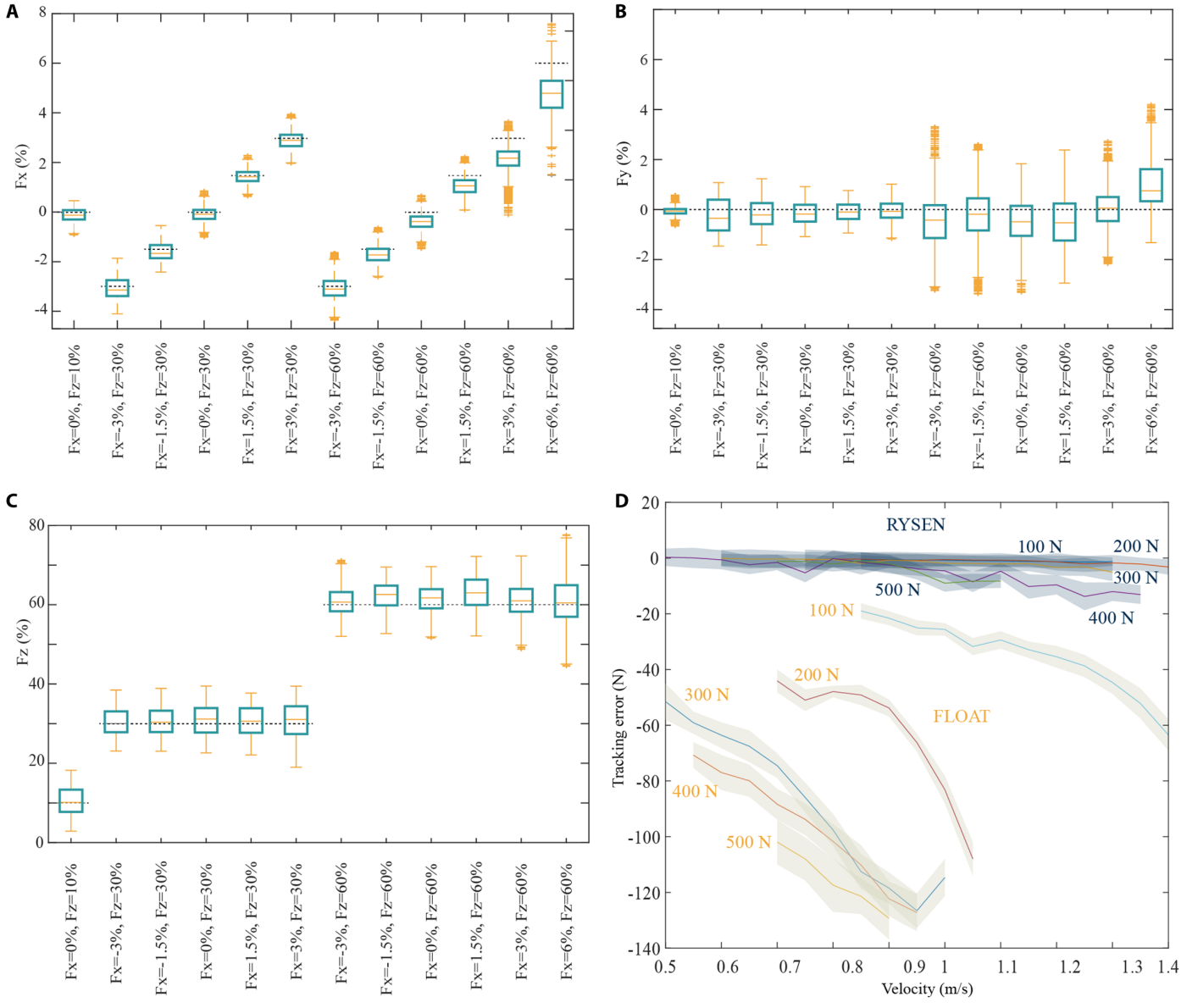

Fig. 2. Force-tracking performance of RYSEN and FLOAT. (**A** to **C**) Force tracking performance of RYSEN in *x*, *y*, and *z* directions during walking with healthy participants in the *x* direction. The force shown is measured by RYSEN. Horizontal lines indicate set points, the central marks of the box plots indicate the median, and the bottom and top indicate the 25th and 75th percentiles. Walking velocity, 0.99 m/s (±0.22). (**D**) Force tracking errors for the AP force of RYSEN and FLOAT as functions of walking velocity and unloading force. The shaded areas show SD. FLOAT values are derived from the data in (*9*).

such that the actually rendered support force vector is close to the reference support force vector. We addressed the two research questions:

2a) Do humans walk most similar to normal walking when the AP force is zero?

2b) Do humans select a zero AP force when given the choice?

As a candidate metric that can widely be used and shows the relationship between AP force and walking, we investigated self-selected walking velocity (*34*–*36*), addressing the questions:

2c) Is there a positive correlation between the AP force and the self-selected velocity?

2d) Is the self-selected velocity with AP force of zero equal to the self-selected velocity without unloading?

For these two questions, we also performed the tests with three individuals with SCI to investigate to what extent the results match those of healthy participants. RYSEN's high transparency allows for generalization of the results in this section across different BWS devices. Results in this section are shown in patient coordinates (AP, lateral, vertical), which align with the device coordinates (*x*, *y*, *z*) in these experiments.

2a. Do humans walk most similar to normal walking when the AP force is zero?

We recorded vertical ground reaction force (GRF) profiles and AP GRF impulse for 15 healthy participants under different unloading conditions and type 2 attachment (see Fig. 1B). The values were normalized by the weight of the respective participant after unloading.

Table 1. Overview on damping parameters for device transparency for RYSEN and FLOAT during walking. FLOAT values are derived from the data in (*9*) and are therefore only available in the *x* direction.

Transparency parameter	RYSEN	FLOAT
Speed while walking with 100-N unloading	0.86 m/s (±0.18)	1.10 m/s (±0.19)
Damping while walking with 100-N unloading	*x*: 2 Ns/m *y*: 24 Ns/m *z*: 288 Ns/m	*x*: 81 Ns/m
Speed while walking with 500-N unloading	0.73 m/s (±0.20)	0.74 m/s (±0.13)
Damping while walking with 500-N unloading	*x*: 3 Ns/m *y*: 50 Ns/m *z*: 299 Ns/m	*x*: 137 Ns/m

Table 2. Overview of the linearized device impedance parameters of RYSEN.

RYSEN device impedance parameter	*x*	*y*	*z*
Linearized mass in *x*, *y*, and *z* directions with 300-N unloading	5.1 kg	2.2 kg	23.5 kg
Linearized damping in *x*, *y*, and *z* directions with 300-N unloading	14 Ns/m	64 Ns/m	224 Ns/m
Linearized stiffness in *x*, *y*, and *z* directions with 300-N unloading	174 N/m	116 N/m	1 N/m
Mean measurement error	−12 N	−14 N	−15 N
Mean tracking error	0 N	−12 N	5 N
Control bandwidth in *x*, *y*, and *z* directions with 300-N unloading	2.2 Hz	2.6 Hz	2.1 Hz

Figure 3D shows the normalized horizontal impulses of healthy participants walking in RYSEN with vertical unloading of 30 and 60% BW and AP forces ranging from −3 to 3% of their BW. It shows that the horizontal impulses vary with the AP force and unloading, with significant differences mainly at −3, 1.5, and 3% AP force. An AP force setting between −1.5 and 0% leads to results most similar to normal walking.

Figure 3B shows the normalized vertical GRF for the 30 and 60% BWS conditions, showing the M-shaped profile resulting from heel-strike and push-off. It shows that with a high positive unloading, the second peak (push-off) disappears. With −3% AP force, the first peak remains. Judging from the graphs, the shape of the vertical GRF at −1.5% AP force most resembles normal walking. This is confirmed by the Euclidean distance between the GRF profiles for different conditions and normal walking: This distance is minimized for the −1.5% condition for both 30 and 60% unloading.

Gait models can supplement experimental investigation of BWS conditions (*37*), and thus, we simulated the muscle-reflex model (*38*) (see fig. S5) with similar BWS conditions. Supporting the human experiments, the model achieved a stable gait for −1.5% AP force and not for any positive AP force. This suggests the necessity of a small negative AP force to achieve a physiologically normal gait.

2b. Do humans select a zero AP force when given the choice?

We let 15 healthy participants walk in RYSEN with 30% vertical force and asked them to adjust the AP force until walking felt most natural. Figure 4A shows the range of self-selected AP forces. These results show that participants select an AP force between −1.5 and −1%. This means that they select an AP force that leads them to walk slower than without BWS, as we will see in the results of research question 2c. The chosen AP forces differ substantially from the values reported in an earlier study with FLOAT, which reached +6% (*9*).

In the trial sessions with the three individuals with SCI, we continuously asked the individuals for an opinion on the force setting and let a physiotherapist assess the walking pattern. On the basis of these two factors, the AP forces deemed best (by therapists) were −1% (participant P1), 0% (participant P2), and +1% (participant P3).

2c. Is there a positive correlation between the AP force and the self-selected velocity?

We recorded the normalized self-selected velocity of 15 participants walking in RYSEN with 60% unloading and an AP force varying between −3 and +3% (Fig. 4A). The figure also shows the same data recorded with FLOAT, extrapolated to the −3 until +3% domain. The data for FLOAT are extrapolated, because FLOAT has a controller bias during walking that leads to negative actual AP forces (see Fig. 2). The figure shows that, on average, humans increase their velocity by 5% per percent-point AP force, independently of the device.

We expected that neurologically impaired individuals would show a similar relationship as healthy participants, although the exact relationship probably differs per participant. Therefore, we let three participants with SCI (see fig. S2 for details) walk in RYSEN with parallel bars, 20% unloading (and 55% for participant P3), and a selection of AP forces. The results (Fig. 4B) do not show such a clear relationship as there was with healthy participants. The velocity of P2 does not show a clear trend, whereas P1 has a maximum around 0 to 1% AP force. Only P3 shows behavior similar to healthy participants.

2d. Is the self-selected velocity with AP force of zero equal to the self-selected velocity without unloading?

The results in Fig. 4D show the self-selected velocity of 15 healthy participants walking without RYSEN and walking in RYSEN with 10 and 60% unloading, all with zero AP force. The three conditions do not differ significantly.

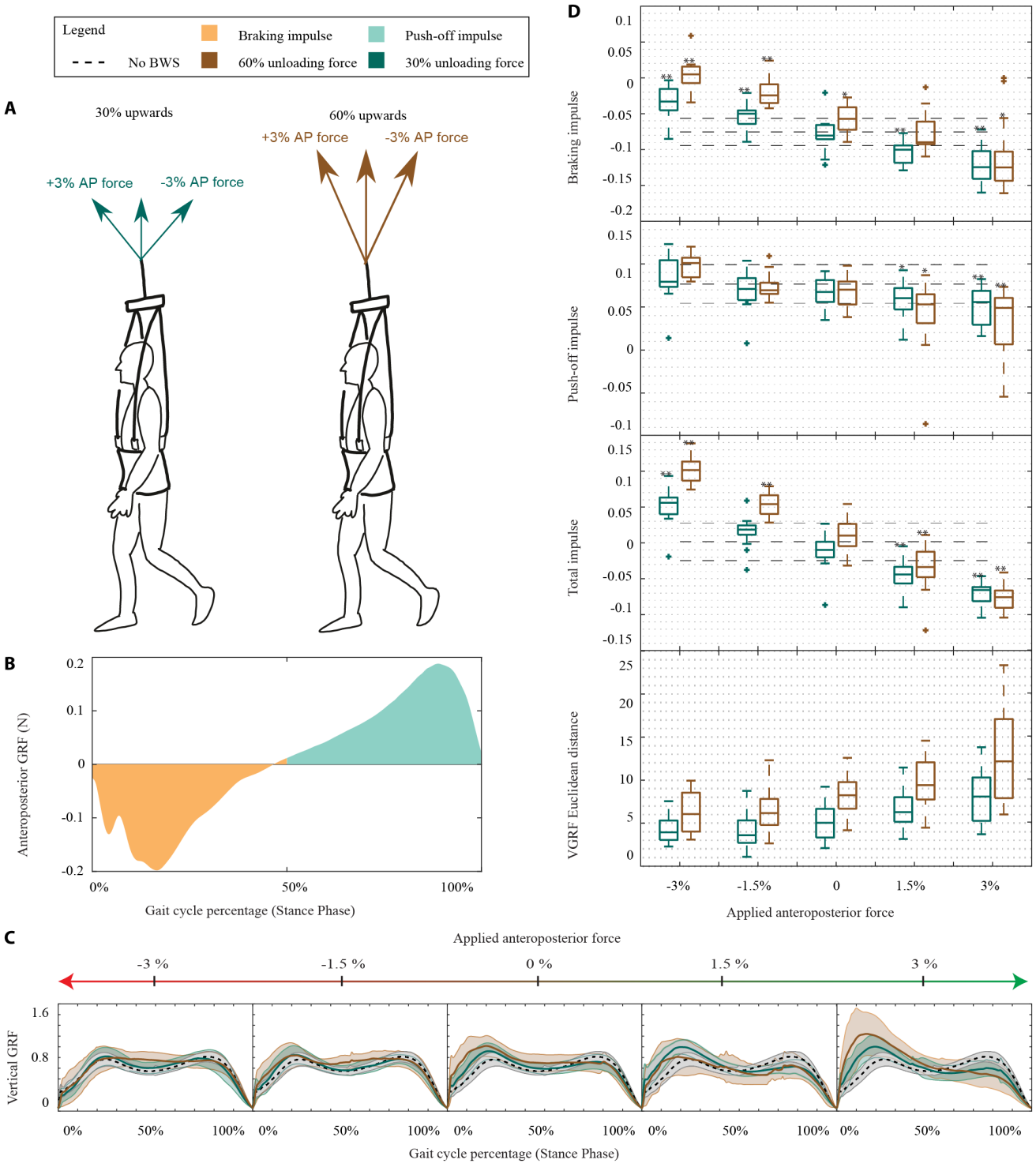

Fig. 3. Vertical GRFs and horizontal impulses for healthy participants with different unloading and AP forces. (**A**) Illustration of the unloading conditions (30 and 60%) and AP forces (−3, 0, and 3% are shown). (**B**) Example for a GRF dataset for walking (type 2 attachment) with indicated braking impulse and push-off impulse. (**C**) Vertical GRF (VGRF) normalized by the full weight of the participant for different AP forces. The shaded areas show SD. (**D**) Braking impulse, push-off impulse, and their sum, i.e., total horizontal impulse, obtained from normalized AP force profile as indicated. Dotted lines indicate mean and SD for the baseline without RYSEN, i.e., 0% unloading condition, and "*" indicates a significant ($P = 0.05$) deviation from this baseline. The bottom plot depicts the Euclidean distance between VGRF profiles for the baseline and the different unloading conditions. The central marks of the box plots indicate the median, and the bottom and top indicate the 25th and 75th percentiles.

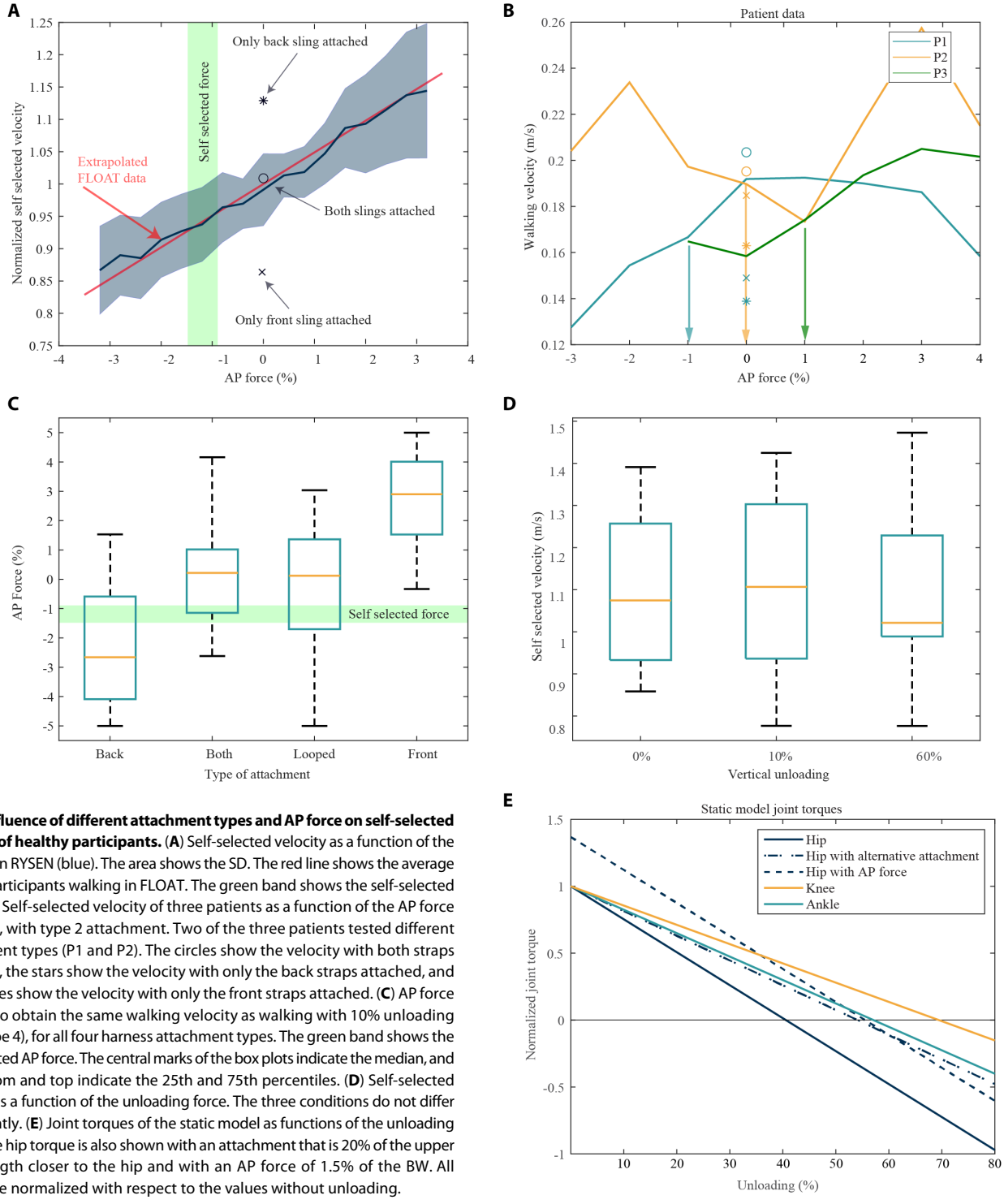

Fig. 4. Influence of different attachment types and AP force on self-selected velocity of healthy participants. (**A**) Self-selected velocity as a function of the AP force in RYSEN (blue). The area shows the SD. The red line shows the average of four participants walking in FLOAT. The green band shows the self-selected force. (**B**) Self-selected velocity of three patients as a function of the AP force in RYSEN, with type 2 attachment. Two of the three patients tested different attachment types (P1 and P2). The circles show the velocity with both straps attached, the stars show the velocity with only the back straps attached, and the crosses show the velocity with only the front straps attached. (**C**) AP force needed to obtain the same walking velocity as walking with 10% unloading force (type 4), for all four harness attachment types. The green band shows the self-selected AP force. The central marks of the box plots indicate the median, and the bottom and top indicate the 25th and 75th percentiles. (**D**) Self-selected velocity as a function of the unloading force. The three conditions do not differ significantly. (**E**) Joint torques of the static model as functions of the unloading force. The hip torque is also shown with an attachment that is 20% of the upper body length closer to the hip and with an AP force of 1.5% of the BW. All values are normalized with respect to the values without unloading.

D3: Attachment to the harness

The attachment of the BWS system to the user-worn harness has rarely been studied, although it determines how the unloading forces are distributed along the body. The line of action of the resultant force applied to the person determines which moments the unloading force applies with respect to joints of the user, and with respect to the body's center of mass. The moment about the center of mass directly influences centroidal angular momentum, a key concept of bipedal stability and often used for balance control of humanoid robots (*21*). Centroidal angular momentum can normally only be manipulated through foot-ground interaction forces, but it can be intensely manipulated or disturbed through moments induced by a BWS force vector. The fact

that the force acts at the upper body drastically changes which joint moments muscles need to generate for the same apparent posture.

We expect that depending on the attachment location (and therefore on the moment arms) the effect of identical forces can differ strongly and influence body posture, gait velocity, kinetic parameters, muscle activity, or metabolic cost.

To analyze the effect of the attachment, we developed a simple static model (see Materials and Methods). Figure 4E shows the model's joint torques as functions of the vertical unloading. The torques change sign at a BWS unloading of 41, 57, and 69% for the hip, knee, and ankle torques, respectively. This change of sign means that the user's muscles no longer hold the upper body up, as necessary for a normal, forward-leaning posture under the influence of gravity, but instead need to pull the upper body in the opposite direction, downward.

Figure 4E also shows the hip torque with an attachment that is 80% of the distance between hip and shoulder. This changes the slope of the hip torque, increasing the unloading where the hip torque changes sign. Furthermore, Fig. 4E shows the hip torque with an AP force of 1.5%. The results show that this increases the hip torque, increasing the unloading where the hip torque changes sign. Both changes have about the same effect on where the hip torque changes sign: This torque increases from 41 to about 55%. Similar increases were observed in knee and ankle torques.

To study the effect of this phenomenon on human participants, we experimentally compared four attachment types (Fig. 1B):

1) The BWS attaches only at the front of the harness.

2) The BWS attaches at both the front and the back of the harness.

3) The BWS attaches only at the back of the harness.

4) The BWS attaches at both the front and the back of the harness, and the attachment slings are looped at the sling bar. This means that when a person is leaning forward, the front strap elongates and the back strap shortens.

Types 1 and 3 are extreme versions of type 2 when the front and back straps are not tightened equally. These types are not used intentionally in practice, but they serve the purpose of showing the influence of the attachment location and strap tightening.

We investigated the influence of these different types on human self-selected velocity. As an example, because of the torque sign change in the static model above, we expect that type 1 impedes locomotion and therefore reduces self-selected velocity. Therefore, we attempt to answer the following questions:

3a) Does an attachment only on the front of the harness (type 1) result in a lower self-selected velocity? And does an attachment only on the back of the harness (type 3) result in a higher self-selected velocity?

3b) Is there a difference in self-selected velocity between a fixed attachment with both straps equally tightened (type 2) and a looped attachment (type 4)?

As the results on question 3a will show, the self-selected velocity changes when the attachment is only the front or back of the harness with respect to both straps attached. This means that different attachment types could lead to different optimal AP force settings. To investigate whether this is the case, we address the following question:

3c) Can the change in self-selected velocity from research question 3a be compensated for by adjusting the AP force?

Results in this section are shown in patient coordinates (AP, lateral, vertical), which align with the device coordinates (x, y, z) in these experiments.

3a. Does an attachment only on the front of the harness (type 1) result in a lower self-selected velocity? And does an attachment only on the back of the harness (type 3) result in a higher self-selected velocity?

We let 15 healthy participants walk with attachment types 1, 2, and 3 and 60% unloading force. Figure 4 shows the average self-selected velocity with only the front sling and only the back sling attached. The results show a statistically significant decrease (type 1) and increase (type 3) in self-selected velocity with respect to a type 2 attachment. The test was repeated with three patients, of whom P3 was unable to walk with these conditions. Both conditions resulted in reduced walking speed.

3b. Is there a difference in self-selected velocity between a fixed attachment with both straps equally tightened (type 2) and a looped attachment (type 4)?

We let 15 healthy participants walk with attachment types 2 and 4 and 60% unloading force while varying the AP force until the self-selected velocity matched their self-selected velocity at 10% unloading and type 4 attachment. Figure 4C shows the AP force required to match the normal self-selected velocity. The two conditions do not differ significantly.

3c. Can the change in self-selected velocity from research question 3a be compensated for by adjusting the AP force?

We let 15 healthy participants walk with attachment types 1 and 3 and 60% unloading force while varying the AP force until the self-selected velocity matched their self-selected velocity at 10% unloading and type 4 attachment. Figure 4C shows the AP force required to match the normal self-selected velocity. The results show that adjusting the AP force can compensate the change in self-selected velocity due to attachment. Logically, only attachment at the front (type 1) requires a positive AP force to compensate.

Results summary

Table 3 summarizes the results of the three determinants.

DISCUSSION

The results above show how humans change their gait in response to interaction with a BWS device. Below, we discuss the three determinants and deliberate the generalizability of the results.

D1: Device transparency

The transparency of RYSEN was presented in detail. The force tracking bandwidths of RYSEN are at least 2 Hz in all three Cartesian directions. This value, being higher than the average walking frequency of healthy humans [i.e., 100 steps/min for moderate-intensity walking (*39*)], indicates that RYSEN is capable of tracking gait phase–dependent forces. However, a bandwidth of 2 Hz does not mean that forces can be reliably tracked up to that point. When a phase shift occurs, this can also be disturbing to a walking person. To reliably render a variable force that depends on the gait phase, it is advisable to add feed-forward terms to the controller, for example, using information from adaptive oscillators or similar concepts (*40*).

The measured transparency was highest in the x direction, followed by the y direction and finally the z direction. These different transparencies are determined by the device configuration. Force sensing in the y direction is also influenced by cable friction, but the gearbox friction of the involved motor is lower. RYSEN is most transparent in the x direction, because force sensing in the x direction

Table 3. Summary of the results.

D1: Transparency	
1. What is the transparency of state-of-the-art 3D BWS systems?	In the most transparent device we measured, the apparent damping was roughly 2–3, 24–50, and 288–299 Ns/m in *x*, *y*, and *z* directions, respectively, during walking. The least transparent device showed damping between 83 and 137 Ns/m in *x* direction.
D2: Support force vector	
2a. Do humans walk most similar to normal walking when the AP force is zero?	No, a negative AP force is required with a transparent device and type 2 harness attachment.
2b. Do humans select a zero AP force when given the choice?	No, they select between −1 and −1.5% AP force for a transparent device and type 2 harness attachment.
2c. Is there a positive correlation between the AP force and the self-selected velocity?	Yes, the velocity increases with about 5% of the normal walking velocity per % AP force.
2d. Is the self-selected velocity with AP force of zero equal to the self-selected velocity without BWS device?	Yes.
D3: Attachment to the harness	
3a. Does an attachment only on the front of the harness (type 1) result in a lower self-selected velocity? And does an attachment only on the back of the harness (type 3) result in a higher self-selected velocity?	Yes, the two conditions show significantly lower (type 1) and higher (type 3) self-selected velocity.
3b. Is there a difference in self-selected velocity between a fixed attachment with both straps equally tightened (type 2) and a looped attachment (type 4)?	No.
3c. Can the change in self-selected velocity from research question 3a be compensated for by adjusting the AP force?	Yes, about 3% AP force in the correct direction can compensate the velocity change due to attachment types 1 and 3.

strongly relies on an inertial measurement unit in the sling bar, which is not particularly influenced by friction.

The magnitude of the tracking error during walking is best shown in Fig. 2A, which shows the tracking errors to be relatively small, except for conditions with 60% BWS. Under those conditions, the force in the *x* direction shows a negative bias, which increases with the reference force in the *x* direction. The largest horizontal bias is 1.2% BW at the 6% BW forward force condition. The largest vertical bias is 3.0% BW. Under all other conditions, bias and variability are small: The horizontal bias is maximally 0.2% BW in the *x* direction and 0.3% BW in the *y* direction, and the vertical bias is maximally 1.2% BW.

Comparison between devices

We analyzed the transparency of FLOAT and RYSEN. The results from RYSEN are discussed above, and the results from FLOAT were obtained from reinvestigating the recorded data from a previous study (*9*), because the FLOAT specimen that was originally used had been dismantled, and there was no transparency information from the manufacturer on it. The characterizations in (*12*, *20*) had been performed with a different FLOAT specimen. In force plate data of (*9*), the impulse associated with the AP foot-ground interaction forces, as measured by the force plates (area under the force-time curve), is not zero when FLOAT is set to apply zero AP forces. This is already visible in the plots shown in (*9*). Because the participants did not systematically speed up or slow down, this impulse must, however, be zero or close to zero, according to Newton's first law. This suggests that FLOAT was applying a net horizontal force in backward direction. This conclusion is supported by the sensing data of FLOAT, which shows that the control bias in FLOAT heavily depended on the walking velocity as shown in Fig. 2D.

From its mechanical design, FLOAT is theoretically able to render vertical forces more precisely than RYSEN, because this degree of freedom (DOF) is purposefully actuated with less bandwidth in RYSEN, for safety and power-saving reasons.

Implications of low and high transparency

For BWS systems with low transparency, therapists can use the reference AP force to compensate for undesired apparent device impedance for a specific point of operation. For example, a constant forward reference force can, in principle, compensate for the effect of undesired apparent damping for a given velocity. However, the undesired interaction forces depend not only on velocity but also on the amount of unloading, as also found in (*20*). The compensation needs adapting whenever the point of operation changes. Because the compensating AP reference forces are device specific, the findings cannot be generalized or compared to other BWS systems.

In contrast, in highly transparent devices, little reference AP force is needed to compensate device impedance, and the reference AP force that is set to achieve a natural gait pattern points to a neuromechanical prerequisite, which can then be generalized to other transparent devices.

This highlights once more the importance of the transparency of a BWS system being known and stated in publications, including remaining impedance and bias force in zero-force control. It is therefore important that the rehabilitation technology community can start using standardized benchmarking methods to characterize different devices and produce comparable research output. When a test bench is available to apply and measure forces at the interaction point of the device, the remaining impedance can be characterized with a method similar to the one used in (*41*, *42*). This is simplified when the device itself is capable of measuring interaction forces and kinematics.

The higher remaining impedance of FLOAT in horizontal directions, compared to RYSEN, explains at least some of the discrepancies in the AP force results discussed in the following section.

D2: Support force vector

AP forces strongly influence kinematics and kinetics of human gait. The current experiments with RYSEN show that the most natural condition emerges from a small negative AP force and that participants also select a small negative AP when given the choice. This seems to challenge the paradigm that humans optimize their motions for energy efficiency (*43*), and there is no indication either that a small negative force is optimal in reducing motor noise (*44*). We hypothesize that there is an optimization goal that supersedes both energy

efficiency (*45*) and noise reduction in the generation of human motion: (perceived) safety.

We see two reasons why small negative AP forces feel safer. First, having to pull the BWS device along increases the feeling of control over the device, whereas with a zero AP force the device seems to move without an interaction force, and with a positive AP force, the device even seems to lead. The negative AP force also reduces gait speed (Fig. 4A); slower speeds increase local dynamic stability (*46*). However, high negative forces increase energy cost of walking and impede gait initiation. Second, a negative AP force favors a forward-leaning posture. Normally, leaning forward reduces the chance of dangerous backward falls. During walking, falling forward can be prevented with a swift movement of the swing leg, but a backward fall cannot be prevented this way (*47*). Therefore, leaning forward increases the margin with respect to falling backward and might be perceived as safer. This feeling of safety is crucial; not only does the fear of falling affect walking patterns in healthy adults but it is also often more detrimental in patients (*48*) or healthy elderly people (*49*). Similarly, we hypothesize that because the task feels safer, walking patterns are closer to normal walking. In future studies, this perceived safety should be assessed for different parameter settings to validate this hypothesis, e.g., with questionnaires and by means of a visual analog scale (*50*) or Likert-type scale (*51*).

From the results of D1 and D2, we conclude that the high values of positive AP force of up to +6% BW (*9*), which can be used in FLOAT to achieve natural gait patterns, are specific to the FLOAT specimen used and, for a large part, compensate device impedance. RYSEN has a lower remaining impedance, and we have not observed a substantial horizontal force bias. Therefore, the reference forces for RYSEN need to compensate less for remaining device impedance and better reflect the actual AP force that an individual requires to walk naturally when being unloaded.

The results on three patients with SCI do not fully align with the results on healthy participants, stressing the importance of the individual neurological condition in determining optimal support. The selected AP forces were slightly higher than those selected by the healthy participants. However, the sample size does not allow for generalization of this result. Furthermore, transferring settings between patients is difficult because patients with different abilities may have different needs.

D3: Attachment to the harness

Although largely neglected in literature as a determinant for walking in BWSs, strap and harness designs strongly influence walking patterns. As evinced in both our static models and experimental results, different attachments can lead to different joint torques and to drastically different walking patterns. Harness attachment can actually make positive AP forces beneficial in one system and detrimental in another. We have not found a significant difference between walking with looped sling (type 4) and four fixed slings (type 2). This suggests that if all four straps are tightened approximately equally, results on a device with looped slings transfer to a device with fixed slings and vice versa.

The static model shows that the sign of joint torques can change due to an unloading force applied at the upper body. Sign inversions in the hip torque could even impede certain individuals from being able to walk. Without BWS, humans can exploit the inverted pendulum effect to bring their center of mass (CoM) in front of their ankle, bringing their center of pressure (CoP) forward to initiate a step. In static cases, while leaning forward, the hip torque is positive, meaning that humans have to actively counteract the gravitational torque on the trunk to prevent having to step forward. A sign inversion eliminates the inverted pendulum effect of the trunk, meaning that humans must actively bring their CoM in front of their ankle to initiate a step. This makes walking more difficult for healthy individuals and even impossible for individuals with limited or no available hip torque. We hypothesize that sign changes in the hip relate to the change in walking pattern that many studies report above 30% support force (*14*).

Sign changes in the knee torque could also impede certain individuals from being able to walk. Without BWS, gravity causes an extending torque in the knee, making it easier to hold the knee extended. Sign changes eliminate this effect, meaning that humans have to actively keep their knee extended in stance phase. This makes walking harder for healthy participants and even impossible for humans with limited or no available knee torque.

Our experiments for research question 3a showed that the attachment influences self-selected walking velocity (Fig. 4A). The experiment for the subsequent research question 3c indicates that for type 1 and type 3 attachments, an increased (type 1) or decreased (type 3) AP force can compensate the change in walking velocity. The experiment for question 3a was also repeated with three patients. Both attachment variations (types 1 and 3) reduced the self-selected walking velocity (Fig. 4D). A possible explanation is that patients, who already have affected walking capabilities, prefer reducing the walking speed in the presence of an unfamiliar attachment type.

Generalization to other BWS devices

For BWS devices with a direct pelvic attachment (e.g., KineAssist) (*52*), the moment arm of the support force to the hip joint is nearly zero. The static model predicts that this is beneficial, because it prevents sign changes in hip torques. However, this is not always possible due to an impaired upper body control caused by some neurological conditions. In such a case, a higher attachment point is beneficial for trunk stabilization, because it produces stabilizing torques around the hip joint. Furthermore, pelvic attachment restricts rotation of the body around the vertical axis, unlike harnesses attached to an overhead suspension point. Thus, depending on the harness fixation, the AP force has to be adapted accordingly.

Another fundamental property of BWS devices is the method used to generate the reference support force and whether this force is intended to be constant or vary with gait phases. Devices based on a counterweight influence gait differently than those with a spring support and/or a feedback-controlled motorized winch (*37*, *53*, *54*). Because gait phase–dependent vertical unloading has shown potential in pilot studies (*14*), extending this approach to AP forces can be a promising direction for future research.

To summarize, therapy settings cannot be transferred between devices without knowing whether device properties are the same, and care needs to be taken when comparing outcomes of therapeutic regimes conducted with different systems. Regardless of these properties, two findings of this study generalize to all BWS devices. First, participants seem well able to judge optimal settings themselves. Instead of choosing no or positive AP forces, participants chose AP forces that made their gait more similar to normal walking. Second, small variations in AP force can strongly affect gait performance (*9*). Therefore, having a device that can precisely render AP forces is necessary to distinguish between participants and to compensate for other device properties such as remaining impedance and harness attachment.

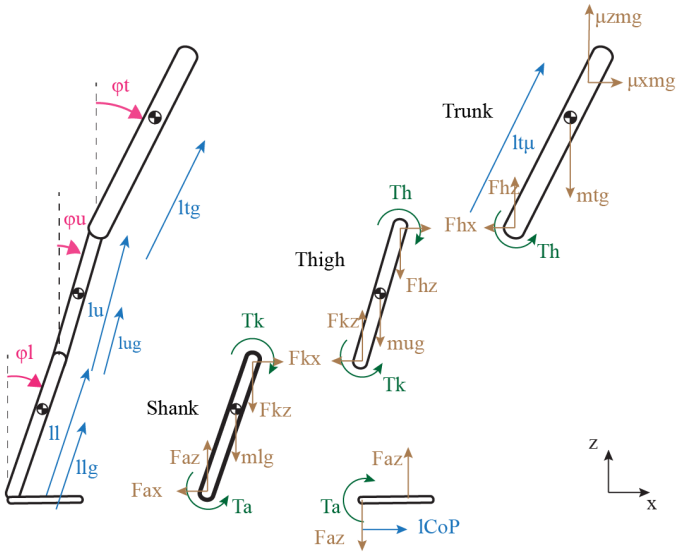

Fig. 5. Definitions and free-body diagrams of the static model of the human body with BWS.

Limitations of this paper

In this work, we only analyzed the vertical and AP GRF parameters and gait velocity. Although gait velocity and the vertical GRF profile are indicators of the functional improvement due to rehabilitation (*55*, *56*), BWS also affects joint moments, pelvic and trunk motion, vertical motion of the center of gravity, etc. Analysis of these kinematic and kinetic parameters and electromyography can help extend this work. Another limitation is the low number of neurologically impaired participants included in the study, as our focus was on validation of the proposed hypotheses for the design of robotic systems and not on conducting a clinical trial. Furthermore, the small negative forces measured in RYSEN might have some compensatory aspects, especially in the *y* direction, where the damping is larger. In addition to the AP direction, investigating the influence of force in the ML direction can allow a more efficient utilization of a 3D BWS device. Last, the AP force was set only in discrete steps of 1.5% for the analysis of GRFs. A higher resolution of AP forces could improve the precision of these results.

CONCLUSION

We evaluated the influence of three determinants on gait when walking with a BWS system:

1) Regarding device transparency, we found large differences between two state-of-the-art 3D BWS systems. This influences the generalizability of the AP forces needed to show a natural walking pattern, and we conclude that device transparency should be reported for future research with BWS systems.

2) For the support force direction, in contrast to earlier research, our investigation with RYSEN shows that, when given the choice, participants select a small negative AP force of −1.5% of the BW. The most likely explanation of the difference between the studies is remaining device impedance. Because RYSEN is quite transparent, we can generalize that humans need a small negative AP force to walk normally when being unloaded. The preference for small negative AP forces could not be seen in all three tested neurologically impaired patients.

3) For the harness, we conclude that especially the location of the attachment on it strongly affects the emerging gait patterns.

We showed that the three determinants strongly affect gait; that despite using apparently similar systems, the scientific data obtained by the devices are not similar; and that recommendations for the optimal therapy settings have to be customized to each device.

We conclude that these determinants may explain the variability in outcomes in neurorehabilitation research, and reporting them will enable comparing results from different devices and eventually help to create evidence for neurorehabilitation principles across devices.

MATERIALS AND METHODS

Objectives and study design

For the three determinants in this study, we used different experiments.

D1: Device transparency

For research question 1, we performed experiments on the linearized dynamic behavior and sensing performance of RYSEN. A dedicated test setup (Appendix: Performance evaluation of the RYSEN) was used to move the end effector of RYSEN while recording interaction forces.

The frequency response of RYSEN was assessed by setting multisine reference forces, with frequencies ranging from 0.4 to 3 Hz. The power of the signals was kept constant over the frequencies, meaning that the amplitudes of the oscillations decreased from 41.8 to 5.6 N in horizontal directions and from 112.8 to 15.0 N in vertical directions.

The linearized remaining impedance was calculated at frequencies between 0.45 and 2.25 Hz (see fig. S3). The motorized slider disturbed the sling bar by applying oscillatory motions. The power was again kept constant, meaning that the amplitudes of the oscillations decreased from 5 cm (0.45 Hz) to 1 cm (2.25 Hz).

Furthermore, we determined RYSEN's dynamic behavior during use with human participants. Fifteen healthy participants walked in RYSEN while recording reference and interaction forces and the position over time. Fifteen other healthy participants walked in RYSEN while recording the GRF, RYSEN interaction force, and position over time.

D2: Support force vector

To answer research questions 2a to 2d, we determined how gait parameters respond to changing unloading level and AP force. Fifteen healthy participants walked in RYSEN while recording GRF, posture, RYSEN interaction force, and position over time. Every participant performed four trials for each of the stated combinations of AP and unloading forces.

This experiment was repeated with three patients with severe chronic SCI with AIS C (American Spinal Injury Association Impairment Scale) (see fig. S2). Patients were enrolled in the STIMO study (ClinicalTrials.gov identifier: NCT02936453) and had completed the intensive rehabilitation training combining spatiotemporal spinal stimulation with robotic BW-supported locomotor training at the time of testing.

Patients were attached to the RYSEN system and were asked to walk overground between parallel bars using their usual spatiotemporal stimulation walking program. The patients were unloaded with 20% (except for P3 who had 55% unloading), and the AP force was initially set to −3% and incrementally increased in 1% steps to +4%. At each AP force level, patients were asked to perform a round trip in the parallel bars (8 m in total) and to give a feedback on the general ease of walking with respect to the current AP force compared to the previous trial. Physiotherapists were also asked to comment on the walking pattern with respect to the different AP forces.

All participants signed informed consent forms, and the experiments were approved by the Delft University of Technology ethics board for the healthy participants and the Swissethics (ethical approval number: PB_2016-00886) for patients. Mathematical descriptions of the metrics used in these experiments can be found in the Supplementary Materials.

D3: Attachment to the harness

A static model was developed to explain how joint torques change with attachment and unloading. Fifteen healthy participants walked in RYSEN while changing the attachment type and AP force and recording the self-selected velocity. Different attachment types were also tested with the three patients mentioned above. The patients were asked to perform a round trip with type 1 attachments and type 3 attachments.

Data acquisition and analysis

We used the setup described in the Supplementary Materials to apply disturbances to RYSEN and to measure the force RYSEN applies. RYSEN data and the external HBM-MCS10 6-DOF force sensor data were recorded at a sample frequency of 1000 Hz.

The participants' self-selected velocity was derived from the time to travel between two predetermined positions within the workspace, using RYSEN position measurements. RYSEN data during those experiments were recorded using a non–real-time recorder with a sample frequency of about 250 Hz. The force references were recorded by hand.

To measure GRFs and participant kinematics, we respectively used synchronized Kistler Type 9260AA6 force plates and a Qualisys Oqus 7+ motion capture system with wearable passive reflective markers. In patient experiments, kinematic analysis was performed offline after 3D reconstruction of the recorded joints (hip, knee, ankle, and foot) to measure walking velocity (in meters per second) in all tested conditions.

In all experiments, participants were not informed up front about the study goal. However, because of obvious differences between many conditions, completely blind testing was impossible. Conditions were randomized between participants, and the data were processed only after all data were collected.

Data were only excluded when participants could not finish the complete experiment. All data were processed in MATLAB. We used the MATLAB implementation of a Welch test for the AP impulse data and two-sample *t* test for all other datasets; a 5% significance level was chosen to test for significant differences.

Static model used for D3

To understand the influence of BWS on the human body, we consider a simple 2D model with ankle, knee, and hip joint (see Fig. 5). BWS in upward and forward direction is modeled as a fraction of human BW, with factors μ_x and μ_z. For static equilibrium, the human joint torques must be (with variables as defined in the free-body diagrams in the figure)

$$T_h = m_t g l_{tg} \sin(\phi_t) - \mu_z mg l_{t\mu} \sin(\phi_t) + \mu_x mg l_{t\mu} \cos(\phi_t) \quad (1)$$

$$T_k = T_h + m_u g l_{ug} \sin(\phi_u) + F_{hz} l_u \sin(\phi_u) + F_{hx} l_u \cos(\phi_u) \quad (2)$$

$$T_a = T_k + m_l g l_{lg} \sin(\phi_l) + F_{kz} l_l \sin(\phi_l) + F_{kx} l_l \cos(\phi_l) \quad (3)$$

We simulated the model with anthropomorphic data (*57*). We averaged between males and females and assumed the trunk, head, arms, and hands to be rigidly connected. This led to a model with $m_t = 40.0$ kg, $m_u = 9.7$ kg, $m_l = 3.1$ kg, $l_l = 0.73$ m, $l_u = 0.40$ m, $l_{lg} = 0.43$ m, $l_{tg} = 0.35$ m, $l_{ug} = 0.24$ m, $l_{lg} = 0.24$ m. We simulated the model with all body segments at an angle of 0.1 rad and the attachment point $l_{t\mu} = 0.53$ m.

SUPPLEMENTARY MATERIALS

www.science.org/doi/10.1126/scirobotics.abf1888
Text
Figs. S1 to S5
Tables S1 to S3

REFERENCES AND NOTES

1. A. Pennycott, D. Wyss, H. Vallery, V. Klamroth-Marganska, R. Riener, Towards more effective robotic gait training for stroke rehabilitation: A review. *J. Neuroeng. Rehabil.* **9**, 65 (2012).
2. H. I. Krebs, N. Hogan, M. L. Aisen, B. T. Volpe, Robot-aided neurorehabilitation. *IEEE Trans. Rehabil. Eng.* **6**, 75–87 (1998).
3. V. Dietz, Body weight supported gait training: From laboratory to clinical setting. *Brain Res. Bull.* **76**, 459–463 (2008).
4. H. Barbeau, M. Visintin, Optimal outcomes obtained with body-weight support combined with treadmill training in stroke subjects. *Arch. Phys. Med. Rehabil.* **84**, 1458–1465 (2003).
5. S. J. Harkema, J. Hillyer, M. Schmidt-Read, E. Ardolino, S. A. Sisto, A. L. Behrman, Locomotor training: As a treatment of spinal cord injury and in the progression of neurologic rehabilitation. *Arch. Phys. Med. Rehabil.* **93**, 1588–1597 (2012).
6. T. George Hornby, D. S. Straube, C. R. Kinnaird, C. L. Holleran, A. J. Echauz, K. S. Rodriguez, E. J. Wagner, E. A. Narducci, Importance of specificity, amount, and intensity of locomotor training to improve ambulatory function in patients poststroke. *Top. Stroke Rehabil.* **18**, 293–307 (2011).
7. C. Krishnan, A. K. Dharia, T. E. Augenstein, E. P. Washabaugh, C. E. Reid, S. R. Brown, R. Ranganathan, Learning new gait patterns is enhanced by specificity of training rather than progression of task difficulty. *J. Biomech.* **88**, 33–37 (2019).
8. J. Hidler, D. Brennan, D. Nichols, K. Brady, T. Nef, ZeroG: Overground gait and balance training system. *J. Rehabil. Res. Dev.* **48**, 287–298 (2011).
9. J.-B. Mignardot, C. G. L. Goff, R. V. D. Brand, M. Capogrosso, N. Fumeaux, H. Vallery, S. Anil, J. Lanini, I. Fodor, G. Eberle, A. Ijspeert, B. Schurch, A. Curt, S. Carda, J. Bloch, J. von Zitzewitz, G. Courtine, A multidirectional gravity-assist algorithm that enhances locomotor control in patients with stroke or spinal cord injury. *Sci. Transl. Med.* **9**, eaah3621 (2017).
10. A. C. Dragunas, K. E. Gordon, Body weight support impacts lateral stability during treadmill walking. *J. Biomech.* **49**, 2662–2668 (2016).
11. D. A. Lawrence, Stability and transparency in bilateral teleoperation. *IEEE Trans. Robot. Autom.* **9**, 624–637 (1993).
12. H. Vallery, P. Lutz, J. V. Zitzewitz, G. Rauter, M. Fritschi, C. Everarts, R. Ronsse, A. Curt, M. Bolliger, Multidirectional transparent support for overground gait training, in *Proceedings of the IEEE 13th International Conference on Rehabilitation Robotics (ICORR)* (IEEE, 2013).
13. M. Plooij, U. Keller, B. Sterke, S. Komi, H. Vallery, J. V. Zitzewitz, Design of RYSEN: An intrinsically safe and low-power three-dimensional overground body weight support. *IEEE Robot. Autom. Lett.* **3**, 2253–2260 (2018).
14. S. Apte, M. Plooij, H. Vallery, Influence of body weight unloading on human gait characteristics: A systematic review. *J. Neuroeng. Rehabil.* **15**, 53 (2018).
15. E. Colgate, N. Hogan, An analysis of contact instability in terms of passive physical equivalents, in *Proceedings of the 1989 International Conference on Robotics and Automation* (IEEE, 1989).
16. H. Vallery, J. Veneman, E. van Asseldonk, R. Ekkelenkamp, M. Buss, H. van Der Kooij, Compliant actuation of rehabilitation robots. *IEEE Robot. Autom. Mag.* **15**, 60–69 (2008).
17. T. Proietti, V. Crocher, A. Roby-Brami, N. Jarrassé, Upper-limb robotic exoskeletons for neurorehabilitation: A review on control strategies. *IEEE Rev. Biomed. Eng.* **9**, 4–14 (2016).
18. N. Jarrassé, T. Proietti, V. Crocher, J. Robertson, A. Sahbani, G. Morel, A. Roby-Brami, Robotic exoskeletons: A perspective for the rehabilitation of arm coordination in stroke patients. *Front. Hum. Neurosi.* **8**, 947 (2014).
19. A. Frisoli, Chapter 6—Exoskeletons for upper limb rehabilitation, in *Rehabilitation Robotics*, R. Colombo, V. Sanguineti, Eds. (Academic Press, 2018).
20. M. Bannwart, M. Bolliger, P. Lutz, M. Gantner, G. Rauter, Systematic analysis of transparency in the gait rehabilitation device the FLOAT, in *Proceedings of the 14th International Conference on Control, Automation, Robotics and Vision (ICARCV)* (IEEE, 2016).

21. A. Goswami, V. Kallem, Rate of change of angular momentum and balance maintenance of biped robots, in *Proceedings of the IEEE International Conference on Robotics and Automation* (IEEE, 2004).
22. E. Berra, R. De Icco, M. Avenali, C. Dagna, S. Cristina, C. Pacchetti, M. Fresia, G. Sandrini, C. Tassorelli, Body weight support combined with treadmill in the rehabilitation of parkinsonian gait: A review of literature and new data from a controlled study. *Front. Neurol.* **9**, 1066 (2019).
23. G. L. Gama, M. L. Celestino, J. A. Barela, L. Forrester, J. Whitall, A. Barela, Effects of gait training with body weight support on a treadmill versus overground in individuals with stroke. *Arch. Phys. Med. Rehabil.* **98**, 738–745 (2017).
24. S. Combs-Miller, A. Kalpathi Parameswaran, D. Colburn, T. Ertel, A. Harmeyer, L. Tucker, A. Schmid, Body weight-supported treadmill training vs. overground walking training for persons with chronic stroke: A pilot randomized controlled trial. *Clin. Rehabil.* **28**, 873–884 (2014).
25. P. W. Duncan, K. J. Sullivan, A. L. Behrman, S. P. Azen, S. S. Wu, S. E. Nadeau, B. H. Dobkin, D. K. Rose, J. K. Tilson, S. Cen, S. K. Hayden, Body-weight–supported treadmill rehabilitation after stroke. *N. Eng. J. Med.* **364**, 2026–2036 (2011).
26. P. R. Lucareli, M. O. Lima, F. P. Lima, J. de Almeida, G. Brech, J. Greve, Gait analysis following treadmill training with body weight support versus conventional physical therapy: A prospective randomized controlled single blind study. *Spinal Cord* **49**, 1001–1007 (2011).
27. C. M. Dean, L. Ada, J. Bampton, M. E. Morris, P. H. Katrak, S. Potts, Treadmill walking with body weight support in subacute non-ambulatory stroke improves walking capacity more than overground walking: A randomised trial. *J. Physiother.* **56**, 97–103 (2010).
28. L. Ada, C. M. Dean, M. E. Morris, J. M. Simpson, P. Katrak, Randomized trial of treadmill walking with body weight support to establish walking in subacute stroke: The MOBILISE trial. *Stroke* **41**, 1237–1242 (2010).
29. L. Ada, C. M. Dean, J. Vargas, S. Ennis, Mechanically assisted walking with body weight support results in more independent walking than assisted overground walking in non-ambulatory patients early after stroke: A systematic review. *J. Physiother.* **56**, 153–161 (2010).
30. E. Swinnen, D. Beckwée, D. Pinte, R. Meeusen, J.-P. Baeyens, E. Kerckhofs, Treadmill training in multiple sclerosis: Can body weight support or robot assistance provide added value? A systematic review. *Mult. Scler. Int.* **2012**, 240274 (2012).
31. C. C. Charalambous, H. S. Bonilha, S. A. Kautz, C. M. Gregory, M. G. Bowden, Rehabilitating walking speed poststroke with treadmill-based interventions: A systematic review of randomized controlled trials. *Neurorehabil. Neural Repair* **27**, 709–721 (2013).
32. J. Mehrholz, S. Thomas, B. Elsner, Treadmill training and body weight support for walking after stroke. *Cochrane Database Syst. Rev.* **2014**, CD002840 (2017).
33. G. Pratt, M. Williamson, Series elastic actuators, in *Proceedings of the 1995 IEEE/RSJ International Conference on Intelligent Robots and Systems. Human Robot Interaction and Cooperative Robots* (IEEE, 1995).
34. M. Cesari, Role of gait speed in the assessment of older patients. *JAMA* **305**, 93–94 (2011).
35. I. G. van de Port, G. Kwakkel, E. Lindeman, Community ambulation in patients with chronic stroke: How is it related to gait speed? *J. Rehabil. Med.* **40**, 23–27 (2008).
36. M. Sekine, T. Tamura, M. Yoshida, Y. Suda, Y. Kimura, H. Miyoshi, Y. Kijima, Y. Higashi, T. Fujimoto, A gait abnormality measure based on root mean square of trunk acceleration. *J. Neuroeng. Rehabil.* **10**, 118 (2013).
37. S. Apte, M. Plooij, H. Vallery, Simulation of human gait with body weight support: Benchmarking models and unloading strategies. *J. Neuroeng. Rehabil.* **17**, 81 (2020).
38. H. Geyer, H. Herr, A muscle-reflex model that encodes principles of legged mechanics produces human walking dynamics and muscle activities. *IEEE Trans. Neural Syst. Rehabil. Eng.* **18**, 263–273 (2010).
39. C. Tudor-Locke, H. Han, E. J. Aguiar, T. V. Barreira, J. M. Schuna Jr., M. Kang, D. A. Rowe, How fast is fast enough? Walking cadence (steps/min) as a practical estimate of intensity in adults: A narrative review. *Br. J. Sports Med.* **52**, 776–788 (2018).
40. C. Everarts, H. Vallery, M. Bolliger, R. Ronsse, Adaptive position anticipation in a support robot for overground gait training enhances transparency, in *Proceedings of the 2013 IEEE 13th International Conference on Rehabilitation Robotics (ICORR)* (IEEE, 2013).
41. F. Sergi, D. Accoto, G. Carpino, N. L. Tagliamonte, E. Guglielmelli, Design and characterization of a compact rotary series elastic actuator for knee assistance during overground walking, in *Proceedings of the 4th IEEE RAS & EMBS International Conference on Biomedical Robotics and Biomechatronics (BioRob)* (IEEE, 2012).
42. F. Parietti, G. Baud-Bovy, E. Gatti, R. Riener, L. Guzzella, H. Vallery, Series viscoelastic actuators can match human force perception. *IEEE/ASME Trans. Mech.* **16**, 853–860 (2011).
43. F. C. Anderson, M. G. Pandy, Dynamic optimization of human walking. *J. Biomech. Eng.* **123**, 381–390 (2001).
44. C. M. Harris, D. M. Wolpert, Signal-dependent noise determines motor planning. *Nature* **394**, 780–784 (1998).
45. D. R. Carrier, C. Anders, N. Schilling, The musculoskeletal system of humans is not tuned to maximize the economy of locomotion. *Proc. Natl. Acad. Sci. U.S.A.* **108**, 18631–18636 (2011).
46. S. A. England, K. P. Granata, The influence of gait speed on local dynamic stability of walking. *Gait Posture* **25**, 172–178 (2007).
47. M. Wisse, A. L. Schwab, R. Q. van der Linde, F. C. van der Helm, How to keep from falling forward: Elementary swing leg action for passive dynamic walkers. *IEEE Trans. Robot.* **21**, 393–401 (2005).
48. V. Jørgensen, E. B. Forslund, A. Opheim, E. Franzén, C. H. Kerstin Wahman, Å. Seiger, A. Ståhle, J. K. Stanghelle, K. S. Roaldsen, Falls and fear of falling predict future falls and related injuries in ambulatory individuals with spinal cord injury: A longitudinal observational study. *J. Physiother.* **63**, 108–113 (2017).
49. K. Makino, H. Makizako, T. Doi, K. Tsutsumimoto, R. Hotta, S. Nakakubo, T. Suzuki, H. Shimada, Fear of falling and gait parameters in older adults with and without fall history. *Geriatr. Gerontol. Int.* **17**, 2455–2459 (2017).
50. A. C. Scheffer, M. J. Schuurmans, N. VanDijk, T. van der Hooft, S. E. D. Rooij, Reliability and validity of the visual analogue scale for fear of falling in older persons. *J. Am. Geriatr. Soc.* **58**, 2228–2230 (2010).
51. E. S. Bower, J. L. Wetherell, C. C. Merz, A. J. Petkus, V. L. Malcarne, E. J. Lenze, A new measure of fear of falling: Psychometric properties of the fear of falling questionnaire revised (FFQ-R). *Int. Psychogeriatr.* **27**, 1121–1133 (2015).
52. J. Patton, D. A. Brown, M. Peshkin, J. J. Santos-Munné, A. Makhlin, E. Lewis, E. J. Colgate, D. Schwandt, KineAssist: Design and development of a robotic overground gait and balance therapy device. *Top. Stroke Rehabil.* **15**, 131–139 (2008).
53. M. K. Aaslund, R. Moe-Nilssen, Treadmill walking with body weight support: Effect of treadmill, harness and body weight support systems. *Gait Posture* **28**, 303–308 (2008).
54. V.-T. Tran, K. Sasaki, S.-I. Yamamoto, Influence of body weight support systems on the abnormal gait kinematic. *Appl. Sci.* **10**, 4685 (2020).
55. R. Dickstein, Rehabilitation of gait speed after stroke: A critical review of intervention approaches. *Neurorehabil. Neural Repair* **22**, 649–660 (2008).
56. T. Takahashi, K. Ishida, D. Hirose, Y. Nagano, K. Okumiya, M. Nishinaga, Y. Doi, H. Yamamoto, Vertical ground reaction force shape is associated with gait parameters, timed up and go, and functional reach in elderly females. *J. Rehabil. Med.* **36**, 42–45 (2004).
57. D. T. Greenwood, *Advanced Dynamics* (Cambridge Univ. Press, 2006).

Acknowledgments: We thank J. van Frankenhuyzen and R. Peuchen for building the evaluation apparatus for force tracking of RYSEN, R. Valette for helping with the healthy participant experiments, J. Ravier for editing the figures and A. Schwab for drawing the sketch of the harness attachments. **Funding:** The work in this paper was partially funded by Eurostars project 10152, by a Marie-Curie career integration grant PCIG13-GA-2013-618899, by Wings for Life accelerated translation program, and by the National Center of Competence in Research (NCCR) Robotics of the Swiss National Foundation. **Author contributions:** M.P., U.K., B.S., J.v.Z., and H.V. were involved in the development of RYSEN. M.P., B.S., and H.V. were involved in the technical evaluation of RYSEN. M.P., G.C., and J.v.Z. were involved in reprocessing FLOAT data from earlier research. S.A., P.B., M.P., and H.V. were involved in the experiments with healthy participants. L.A., G.C., and J.v.Z. were involved in patient experiments. M.P. developed the static model. S.A. performed the muscle-reflex model simulations and processed and analyzed the force plate data from experiments with healthy participants. All authors were involved in discussions on research design and interpretation of results. M.P., S.A., and U.K. drafted the manuscript, with inputs from J.v.Z., H.V., and G.C. on outline and structure. All authors revised it critically, approved the final version, and agreed to be accountable for all aspects of this work. **Competing interests:** During the research presented in this paper, M.P. and B.S. worked (partly) at Motek Medical. J.v.Z. and G.C. are founders and shareholders at Onward Medical (former GTX Medical). G.C. is consultant and board member for Onward Medical. U.K. and J.v.Z. work (partly) at Onward Medical. Both companies, Motek and Onward Medical, benefit from the commercialization of RYSEN. H.V., J.v.Z., G.C., and M.P. are also inventors on multiple patents relating to RYSEN and/or to FLOAT, and may financially benefit from sales of either of these devices through intellectual property (IP) fees. **Data and materials availability:** All data needed to evaluate the conclusions in the paper are present in the paper or the Supplementary Materials. The data and code for this paper can be downloaded here: https://doi.org/10.4121/15059439.

Submitted 19 October 2020
Accepted 26 August 2021
Published 22 September 2021
10.1126/scirobotics.abf1888

Citation: M. Plooij, S. Apte, U. Keller, P. Baines, B. Sterke, L. Asboth, G. Courtine, J. von Zitzewitz, H. Vallery, Neglected physical human-robot interaction may explain variable outcomes in gait neurorehabilitation research. *Sci. Robot.* **6**, eabf1888 (2021).

Science Robotics

Neglected physical human-robot interaction may explain variable outcomes in gait neurorehabilitation research

M. Plooij, S. Apte, U. Keller, P. Baines, B. Sterke, L. Asboth, G. Courtine, J. von Zitzewitz, and H. Vallery

Sci. Robot. **6** (58), eabf1888. DOI: 10.1126/scirobotics.abf1888

Science Robotics (ISSN 2470-9476) is published by the American Association for the Advancement of Science. 1200 New York Avenue NW, Washington, DC 20005. The title *Science Robotics* is a registered trademark of AAAS.